Two novel decamethyl henicosanes (C31H64) identified in a Maoming Basin shale, China

Article *in* Organic Geochemistry · September 2018

DOI: 10.1016/j.orggeochem.2018.09.012

CITATION
1

READS
68

7 authors, including:

Jing Liao
Chinese Academy of Sciences
7 PUBLICATIONS **21** CITATIONS
SEE PROFILE

Lu Hong
Chinese Academy of Sciences
57 PUBLICATIONS **649** CITATIONS
SEE PROFILE

Qiao Feng
Shandong University of Science and Technology
23 PUBLICATIONS **118** CITATIONS
SEE PROFILE

Youping Zhou
Shaanxi University of Science & Technology, Xi'an. CHINA
20 PUBLICATIONS **514** CITATIONS
SEE PROFILE

Organic Geochemistry 125 (2018) 212–219

Contents lists available at ScienceDirect

Organic Geochemistry

journal homepage: www.elsevier.com/locate/orggeochem

Two novel decamethylhenicosanes ($C_{31}H_{64}$) identified in a Maoming Basin shale, China

Jing Liao [a,b], Hong Lu [a,*], Qiao Feng [b], Youping Zhou [c,*], Quan Shi [d], Ping'an Peng [a], Guoying Sheng [a]

[a] State Key Laboratory of Organic Geochemistry, Guangzhou Institute of Geochemistry and Institutions of Earth Science, Chinese Academy of Sciences, Guangzhou 510640, China
[b] Shandong Provincial Key Laboratory of Depositional Mineralization and Sedimentary Minerals, Shandong University of Science and Technology, Qingdao 266000, China
[c] Isotopomics in Chemical Biology & Shaanxi Key Laboratory of Chemical Additives for Industry, School of Chemistry & Chemical Engineering, Shaanxi University of Science & Technology, Xi'an 710021, China
[d] State Key Laboratory of Heavy Oil Processing, China University of Petroleum, Beijing 102249, China

ARTICLE INFO

Article history:
Received 10 November 2017
Received in revised form 11 September 2018
Accepted 18 September 2018
Available online 19 September 2018

Keywords:
Maoming oil shale
NMR
Decamethylhenicosanes
Botryococcus braunii

ABSTRACT

Two new C_{31} branched alkanes (botryococcanes) presumably produced by the B race of *Botryococcus braunii* were isolated and purified from the Maoming Basin shales using column chromatography and preparative gas chromatography and structurally characterized with HR-EI-MS and 1D and 2D NMR. Interpretation of their EI mass spectral and 1D and 2D NMR (HMBC and HSQC) data led to the firm assignments of the two alkanes as diastereoisomeric 2,3,6,7,10,12,15,16,19,20-decamethylhenicosanes (DMHs). The structural assignments were further confirmed by the close match of the measured ^{13}C NMR chemical shifts with those predicted by Lindeman-Adams ^{13}C chemical shift modeling. The skeletons of these two DMHs are virtually identical to that of the recently identified C_{33} botryococcane/botryococcanone in the same sample. It is proposed that these two DMHs share a precursor C_{33} botryococcene biochemically formed by condensing two farnesyl diphosphates involving an unusual cyclobutanation, a retro-Prins reaction and a tetramethylation. A photo-mediated geochemical oxidation of the double bond in the ethenyl group connected to the sole quaternary carbon C-10 is also proposed to be responsible for the formation of the co-occurring DMHs and C_{33} botryococcane/botryococcanone.

1. Introduction

Botryococcanes are the geochemically saturated botryococcenes produced by the B race of the freshwater alga *Botryococcus braunii* (Moldowan and Seifert, 1980; Brassell et al., 1986; McKirdy et al., 1986; Volkman, 2014) and as important biomarkers, carry useful depositional environmental and geological age information (Philp and Lewis, 1987; Guy-Ohlson, 1992; Volkman, 2014). In the Chinese Maoming Basin oil shale and sediments, abundant botryococcanes with "normal" carbon skeletons (where no substituents exist at positions α or β to the sole quaternary carbon C-10) have been reported since 1980s (Fu et al., 1985; Brassell et al., 1986). Subsequently, we have recently identified a C_{33} botryococcane and a C_{33} botryococcan-24-one from a sample collected from the same oil shale formation with an unusual skeleton where a methyl group is β-positioned to the sole quaternary carbon C-10 and we proposed a new biogeochemical pathway for the occurrence of these two new biomarkers in the oil shale (Liao et al., 2018).

When acquiring low resolution mass spectra of the saturated fraction by GC–MS, two well separated peaks in the total ion chromatogram (DMH-1 and DMH-2 marked with asterisks in Fig. 1; see also Supplementary Fig. S1) eluting before the identified C_{33} botryococcane (Liao et al., 2018) attracted our attention. The mass spectra of these two compounds were essentially identical, containing a prominent ion at *m/z* 434, in addition to ions at *m/z* 308, 253 and 281, all characteristic of a botryococcanoid skeleton, (Fig. 1), in particular the novel C_{33} botryococcane and C_{33} botryococcan-24-one (Liao et al., 2018). We suspect these the two compounds represented by these two peaks were genetically related to the C_{33} botryococcane. We therefore isolated and purified, using column chromatography and preparative gas chromatography and structurally characterize these two compounds with a combination of HR-EI-MS, and 1D and 2D NMR techniques. We report here the

* Corresponding authors at: State Key Laboratory of Organic Geochemistry, Guangzhou Institute of Geochemistry and Institutions of Earth Science, Chinese Academy of Sciences, 636 Biaoben Building, 511 Kehua Street, Tianhe District, Guangzhou 510640, China (H. Lu). Isotopomics in Chemical Biology & Shaanxi Key Laboratory of Chemical Additives for Industry, School of Chemistry & Chemical Engineering, Shaanxi University of Science & Technology, 418 Shixun Building, Xianqing Avenue, Weiyang District, Xi'an 710021, China (Y. Zhou).

E-mail addresses: luhong@gig.ac.cn (H. Lu), youping.zhou@sust.edu.cn (Y. Zhou).

https://doi.org/10.1016/j.orggeochem.2018.09.012
0146-6380/

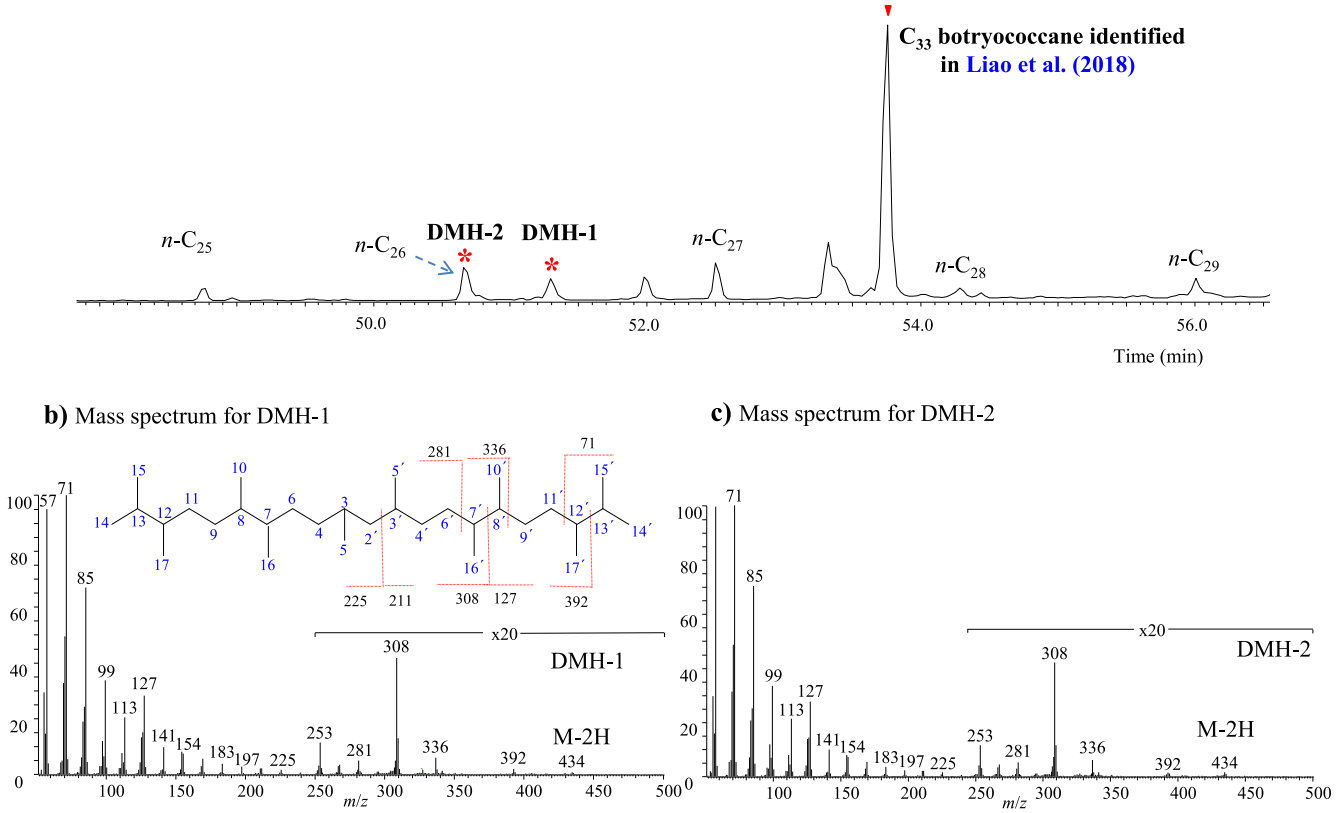

Fig. 1. Segment from the total ion chromatogram (TIC) of saturated hydrocarbon fraction from: (a) the studied Maoming sample; (b) mass spectrum together with the assignment of fragment ions for DMH-1. For clarity, the assignment of fragment ions for the left part of the structure is omitted as the molecular has a perfect centro-symmetry; (c) mass spectrum for DMH-2.

complete elucidation of their structures and discuss the pathway leading to their co-occurrence with the C_{33} botryococcane and C_{33} botryococcan-24-one in the Maoming Basin oil shale sediments.

2. Material and methods

2.1. Sample preparation, target compound isolation and purification

The Eocene sediment sample used in this study was collected from an outcrop of the Maoming Basin located in the southwest part of Guangdong Province, China. Detailed geological and geochemical background information for the sediment sample and sample pretreatment can be found in Liao et al. (2018). Briefly, the sample was ground and Soxhlet-extracted with CH_3OH/CH_2Cl_2 (1:9, v/v) for 72 h. The asphaltene fraction was centrifugally removed by precipitation in *n*-hexane. The maltene fraction was further separated into saturated, aromatic and polar fractions on a silica-aluminium oxide column (0.3 m × 1 cm), with sequential elution with *n*-hexane (80 mL), *n*-hexane/dichloromethane (1:1, v/v, 40 mL) and methanol (40 mL).

The saturated hydrocarbon fraction was subjected to preparative gas chromatography (PGC) (Özek and Demirci, 2012; Zuo et al., 2013) on an Agilent 7890 gas chromatograph interfaced to a Gerstel-preparative fraction collector (PFC), similar to that described by Eglinton et al. (1996). High purity helium (He) was used as a carrier gas at a flow rate of 3.0 mL/min. A DB-5 column (60 m × 0.53 mm × 1.5 μm film thickness) was used to separate and purify the target compounds. The column temperature was held at 80 °C for 2 min, then programmed to 300 °C at 30 °C/min, and held for 40 min. The isolated compounds were weighed (2.8 and 2.6 mg, respectively) and purity confirmed by GC–MS and GC-FID analysis as greater than 95% (Supplementary Fig. S2). The purified target compounds were then subjected to high-resolution mass spectrometry (HR-MS), and nuclear magnetic resonance spectroscopy (NMR) for structural assignment.

2.2. Instrumental analysis

^1H and ^{13}C NMR spectral analyses were conducted on a Bruker AVANCE III 600 MHz NMR spectrometer (operating at 600.19 MHz for ^1H NMR and 150.92 MHz for ^{13}C NMR). Spectra were recorded in $CDCl_3$ solutions, with TMS as internal standard. ^1H NMR chemical shifts were referenced relative to the residual proton signal (7.26 ppm) while ^{13}C NMR chemical shifts were referenced to the central line of the ^{13}C multiplet (77.0 ppm) of $CDCl_3$. A combination of 1D and 2D experiments ^1H-^1H correlation spectroscopy (COSY), heteronuclear single quantum coherence (HSQC), and heteronuclear multiple bond correlation (HMBC) were performed to assign the individual resonances. Distortionless enhanced polarization transfer (DEPT) spectra were used to determine the multiplicity of each ^{13}C nucleus.

GC–MS analysis was performed on a Trace Ultra GC interfaced with a Thermo DSQ-II mass spectrometer operating at 70 eV with a mass range of *m/z* 50–600. A HP-5 column (30 m × 0.25 mm × 0.25 μm film thickness) was used. The oven temperature was programmed from 80 °C (2 min) to 295 °C (25 min) at a rate of 4 °C/min. High purity helium was used as the carrier gas with a constant flow of 1.2 mL/min.

High resolution electron impact mass spectrometry (HR-EI-MS) analysis was performed on a Thermo Finnigan MAT95XP mass spectrometer to determine the accurate mass of the target

compounds. The HR-MS system was operated in the electron impact ionization mode (42 eV) at a resolution of R > 10,000 (10% valley).

Time of flight mass spectrometry (TOFMS) was performed on a Waters GCT Premier. The FI emitter (from CarboTech) of the field ionization-time of flight mass spectrometer (FI-TOFMS) consisted of a 5 μm tungsten wire on which micro carbon needles formed. The emitter (at ground voltage) was located 1.5 mm from a pair of high potential (−12 kV) extraction rods, producing high electric fields (10^{-7}–10^{-8} V/cm) around the tips of the carbon dendrites. The FI emitter current was set at 0 mA during the scan. The emitter was flashed by a current of 7 mA during a 0.3 s interscan cycle to regenerate the emitter. The heater current was 2500 mA.

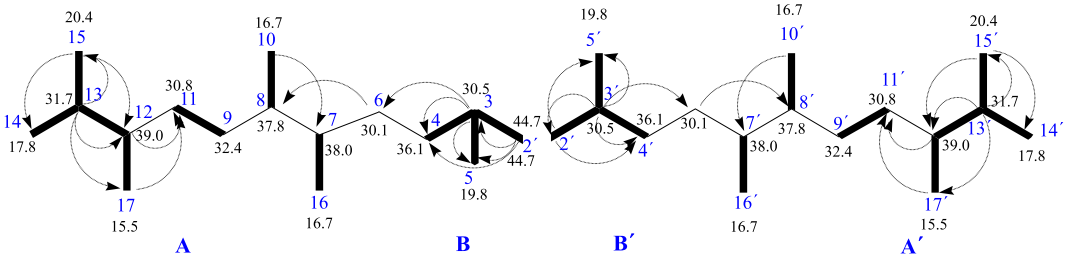

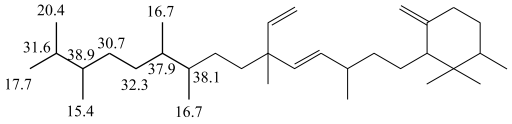

b) sacredicene from Huang et al. (1995)

Fig. 2. (a) Interpretation of key ^{1}H-^{1}H COSY (bold bonds) and HMBC (arrows) correlations (^{1}H → ^{13}C) of DMH-1; (b) Sacredicene from Huang et al. (1995), the left substructure was the same as substructures A and A′ of DMH-1. The numbers in blue are the same used for compounds **1**–**10** in Fig. 7 while those in black are the chemical shifts. (For interpretation of the references to colour in this figure legend, the reader is referred to the web version of this article.)

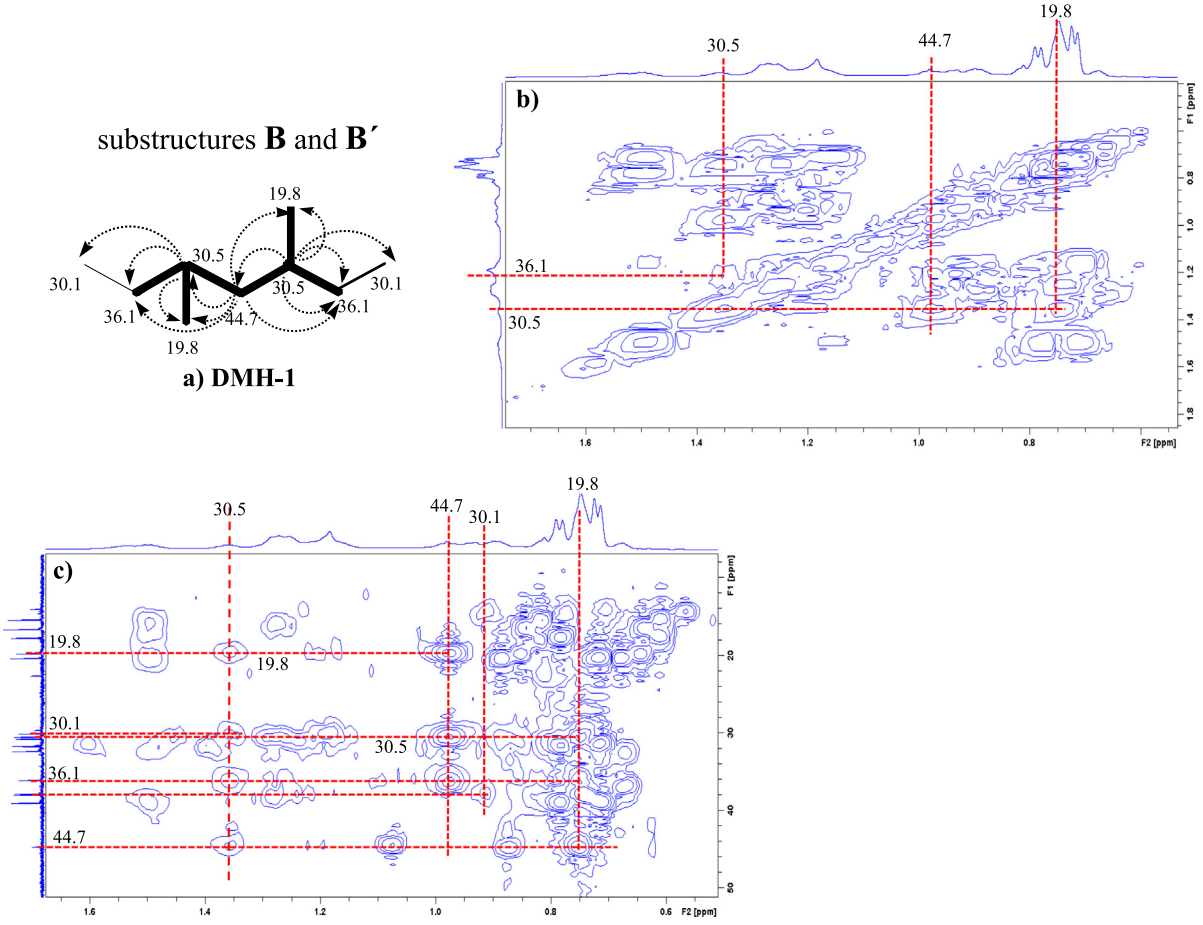

Fig. 3. Assignment for the novel moiety (a) in DMH-1 using (b) ^{1}H-^{1}H COSY and (c) HMBC spectra.

2.3. Lindeman-Adams chemical shift modeling

In ^{13}C NMR, the chemical shift of a nuclei is determined by its local electronic environment in the molecule (Lindeman and Adams, 1971). Strong correlations therefore must exist between the chemical shift and the (local) structure of a molecule. The chemical shifts of the four classes (primary, secondary, tertiary and quaternary) of carbon atoms sub-grouped based on the number of nearest (α), next-nearest (β), the third nearest (γ) and the fourth nearest (Δ) carbon atoms can be predicted from the model of Grant and Paul (1964) or an improved version of it by Lindeman and Adams (1971). Here we use Lindeman-Adams modelling to confirm the new structure proposed in this study. According to their empirical formula, the chemical shift δ_C (k) of the k^{th} C in a molecule can be calculated using: $\delta_C(k) = B_s + \sum_{M=2}^{4}(D_M A_{SM}) + \gamma_s N_{k3} + \Delta_s N_{k4}$, where B_s is the carbon class-dependent parameter, while A_{SM}, γ_s and Δ_s are parameters related to the type of the nearest, the third nearest and fourth nearest carbon atoms to a particular carbon respectively; D_M, N_{k3}, and N_{k4} are the number of the nearest, the third nearest and the fourth nearest carbon atoms, respectively. The values of B_s, A_{SM}, γ_s, and Δ_s can be found in the Table II of Lindeman and Adams (1971).

3. Results and discussion

3.1. Structural identification of DMH-1 and DMH-2

HR-EI-MS analysis of DMH-1 gave an accurate mass at *m/z* 436.5003, in agreement with the calculated value of 436.5008 for the formula of $C_{31}H_{64}$ (Supplementary Fig. S3). The FI-TOFMS spectrum (Supplementary Fig. S4) also confirmed the molecular mass and formula.

The ^{13}C NMR spectrum of DMH-1 (Fig. 5a; see also Supplementary Fig. S6) contained 16 resonances which can be ascribed to 6 CH_3, 5 CH_2 and 5 CH according to the DEPT experiment (Supplementary Fig. S7). Since there are 31 carbons in DMH-1, it is reasonable to assume at this stage that it has 15 pairs of carbons centered symmetrically around one carbon in its skeleton, i.e., there exists a 16-carbon substructure in the skeleton.

To elucidate the structure of DMH-1, we first examined the 2D NMR data (see ^1H-^1H COSY and ^1H-^{13}C HMBC spectra in Fig. 3; HSQC spectrum in Supplementary Fig. S8; an interpretation of the NMR data is displayed in Fig. 2a). ^1H-^1H COSY cross peaks between H-13 and H-12, H-14, H-15 established the C-13/C-12, C-13/C-14, and C-13/C-15 connections, which were confirmed by the HMBC ($^1H \rightarrow {}^{13}C$) correlations from H-15 to C-12 and C-14. Cross peaks between H-12 and H-17 and HMBC correlations from H-13 to C-17 indicated that C-17 was attached to C-12. HMBC and COSY experiments also established the correlations (Fig. 2a) between the methylene carbon C-11 and the methylene carbon C-9 and the methine carbon C-12. Cross peaks between H-8 and H-10, H-7 and H-16 indicated that the methyl carbons C-10 and C-16 were bound to C-8 and C-7, respectively. The HMBC correlations from H-10 to C-7 suggested that C-7 is bound to C-8. Taken together, a substructure **A** (Fig. 2a) can be established for DMH-1. This substructure **A** was essentially the same as the left moiety of the skeleton of the monocyclic C_{33} sacredicene (Fig. 2b) identified in Sacred Lake sediments in Kenya (Huang et al., 1995). The identification of this substructure **A** is further corroborated by

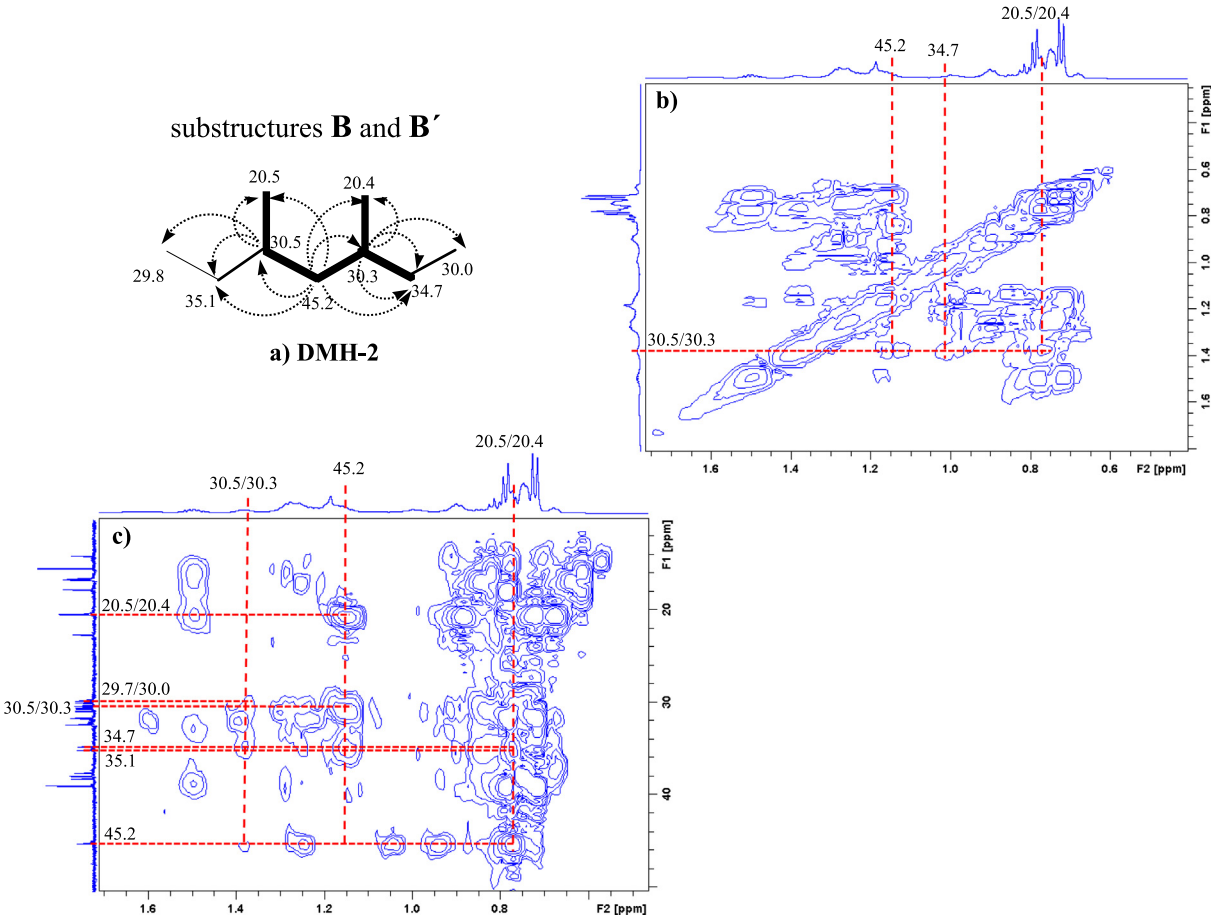

Fig. 4. Assignment for the novel moiety (a) in DMH-2 using (b) ^1H-^1H COSY and (c) HMBC spectra.

Table 1
^{1}H (600 MHz) and ^{13}C (150 MHz) NMR data for the DMH-1 and DMH-2 recorded in $CDCl_3$ and their pairwise δ_C differences.

DMH-1						Pairwise δ_C (ppm) difference	DMH-2					
C. No.	^{1}H, δ (ppm), multiplicity (*J* in Hz)	^{13}C, δ (ppm), multiplicity	DEPT	HMBC ($^{1}H \rightarrow {}^{13}C$)	COSY cross peak		C. No.	^{1}H, δ (ppm), multiplicity (*J* in Hz)	^{13}C, δ (ppm), multiplicity	DEPT	HMBC ($^{1}H \rightarrow {}^{13}C$)	COSY cross peak
3	1.36, m	30.5, d	CH	2′, 5	0.75, 0.98, 1.20	0	3	1.38, m	30.5, d	CH	2′, 5	0.78, 1.15
4	1.20, overlap; 0.94, overlap	36.1, t	CH_2	2′, 3, 5	1.36	**1**	4	1.26, overlap; 0.90, overlap	35.1, t	CH_2	2′, 3, 5	
5	0.75, overlap	19.8, q	CH_3	2′, 3	1.36	−**0.7**	5	0.78, overlap	20.5, q	CH_3	2′, 3	1.38
6	1.26, overlap; 0.93, overlap	30.1, t	CH_2	3		0.3	6	1.18, overlap; 0.99, overlap	29.8, t	CH_2	3	
7	1.25, overlap	38.0, d	CH	10	0.74	−0.2	7	1.25, overlap	38.2, d	CH	10	0.74
8	1.25, overlap	37.8, d	CH	6	0.74	−0.1	8	1.25, overlap	37.9, d	CH	6	0.74
9	1.28, overlap; 0.89, overlap	32.4, t	CH_2			0	9	1.29, overlap; 0.90, overlap	32.4, t	CH_2		
10	0.74, overlap	16.7, q	CH_3		1.25	0	10	0.74, overlap	16.7, q	CH_3		1.25
11	1.28, overlap; 0.89, overlap	30.8, t	CH_2	12, 17		0.2	11	1.28, overlap; 0.89, overlap	30.6, t	CH_2	12, 17	
12	1.16, m	39.0, d	CH	13, 15	0.72, 1.49	0	12	1.16, m	39.0, d	CH	13, 15	0.72, 1.50
13	1.49, m	31.7, d	CH		0.72, 0.78, 1.16	0	13	1.50, m	31.7, d	CH		0.72, 0.79, 1.16
14	0.72, d(6.30)	17.8, q	CH_3	15	1.49	0.1	14	0.72, d(6.72)	17.7, q	CH_3	15	1.50
15	0.78, d(6.66)	20.4, q	CH_3	13	1.49	0	15	0.79, d(6.66)	20.4, q	CH_3	13	1.50
16	0.74, overlap	16.7, q	CH_3		1.25	0.2	16	0.74, overlap	16.5, q	CH_3		1.25
17	0.72, d(6.30)	15.5, q	CH_3	13	1.16	0	17	0.72, d(6.72)	15.5, q	CH_3	13	1.16
2′	0.98, m	44.7, t	CH_2	3, 3′, 5, 5′	1.36	−**0.5**	2′	1.15, overlap; 0.85, m	45.2, t	CH_2	3, 3′, 5, 5′	1.38
3′	1.36, m	30.5, d	CH	5′	0.75, 0.98, 1.20	0.2	3′	1.38, m	30.3, d	CH	5′	0.77, 1.00, 1.15
4′	1.20, overlap; 0.94, overlap	36.1, t	CH_2	2′, 3′, 5′	1.36	**1.4**	4́	1.15, overlap; 1.00, overlap	34.7, t	CH_2	2′, 3′, 5′	
5′	0.75, overlap	19.8, q	CH_3	2′, 3′	1.36	−**0.6**	5́	0.77, overlap	20.4, q	CH_3	2′, 3′	1.38
6′	1.26, overlap; 0.93, overlap	30.1, t	CH_2	3′		0.1	6́	1.27, overlap; 0.90, overlap	30.0, t	CH_2	3′	
7′	1.25, overlap	38.0, d	CH	10′	0.74	0.4	7́	1.25, overlap	37.6, d	CH	10′	0.74
8′	1.25, overlap	37.8, d	CH	6′	0.74	−0.1	8́	1.25, overlap	37.9, d	CH	6′	0.74
9′	1.28, overlap; 0.89, overlap	32.4, t	CH_2			0	9́	1.29, overlap; 0.90, overlap	32.4, t	CH_2		
10′	0.74, overlap	16.7, q	CH_3		1.25	0	10́	0.74, overlap	16.7, q	CH_3		1.25
11′	1.28, overlap; 0.89, overlap	30.8, t	CH_2	12′, 17′		−0.1	11́	1.28, overlap; 0.89, overlap	30.9, t	CH_2	12′, 17′	
12′	1.16, m	39.0, d	CH	13′, 15′	0.72, 1.49	0	12́	1.16, m	39.0, d	CH	13′, 15′	0.72, 1.50
13′	1.49, m	31.7, d	CH		0.72, 0.78, 1.16	0	13́	1.50, m	31.7, d	CH		0.72, 0.79, 1.16
14′	0.72, d(6.30)	17.8, q	CH_3	15′	1.49	0	14́	0.72, d(6.72)	17.8, q	CH_3	15′	1.50
15′	0.78, d(6.66)	20.4, q	CH_3	13′	1.49	0	15́	0.79, d(6.66)	20.4, q	CH_3	13′	1.50
16′	0.74, overlap	16.7, q	CH_3		1.25	0	16́	0.74, overlap	16.7, q	CH_3		1.25
17′	0.72, d(6.30)	15.5, q	CH_3	13′	1.16	0	17́	0.72, d(6.72)	15.5, q	CH_3	13′	1.16

the less than 0.2 ppm position-specific chemical shift discrepancies between the two compounds (Fig. 2a and b).

Examination of the HMBC and ^{1}H-^{1}H COSY experiment also established the correlations (Figs. 2a and 3) between the methine carbon C-3 and the two methylene carbons C-2′ and C-4, the methyl carbon C-5 and between C-4 and C-6. Thus, a substructure **B** could be established. Furthermore, as the HMBC correlation from H-6 to C-8 indicated that C-8 was bound at C-7, substructure **B** must be connected to substructure **A** via a C-6/C-7 bond. Taken together, this novel compound DMH-1 is a symmetrical molecule with the symmetrical center on C2′ and two symmetrical substructures (**A** + **B**) and (**A'** + **B'**) as shown in Fig. 2a. Since it has 21 carbons in the backbone and 10 methyl groups attached to the backbone, this C_{31} hydrocarbon corresponds to 2,3,6,7,10,12,15, 16,19,20-decamethylhenicosane (see **14** in Fig. 7 for the IUPAC naming).

The NMR-based assignment of the structure for DMH-1 is also supported by the mass spectrum of DMH-1 (Fig. 1b): the two weak ions *m/z* 434 and *m/z* 392 are interpreted as a (double) deprotonated molecular ion *m/z* 436 $[M\text{-}2H]^{+\cdot}$ and the neutral loss of the two symmetrical isopropyl groups at the two ends of the backbone. The prominent characteristic ion at *m/z* 308 $[M\text{-}C_9H_{20}]^{+\cdot}$ is believed to be the result of a cleavage of the C-7/C-8 and C-7′/C-8′ bonds. The base ion at *m/z* 71 (C_5H_{11}) is interpreted to be the result of the cleavage of C-12/C-11 and C-12′/C-11′ bonds. Other ions at *m/z* 127, 211, 225, 281, and 336 can also be assigned to the cleavages of relevant chemical bonds as shown in Fig. 1b.

The mass spectrum of DMH-2 (Fig. 1c) is nearly identical to that of the DMH-1 (Fig. 1b) suggesting these two compounds have very similar structures. The ^{13}C NMR spectrum of DMH-2 contained 29 resonances (Fig. 5b and Supplementary Fig. S9) which can be ascribed to 11 CH_3, 9 CH_2 and 9 CH according to the DEPT experiment (Supplementary Fig. S10). Since there are 31 carbons in the DMH-2 according to the FI-TOFMS analysis (Supplementary Fig. S5), resonances for two of the 31 carbons must have overlapped with other resonances (resonances at 39.0 ppm and

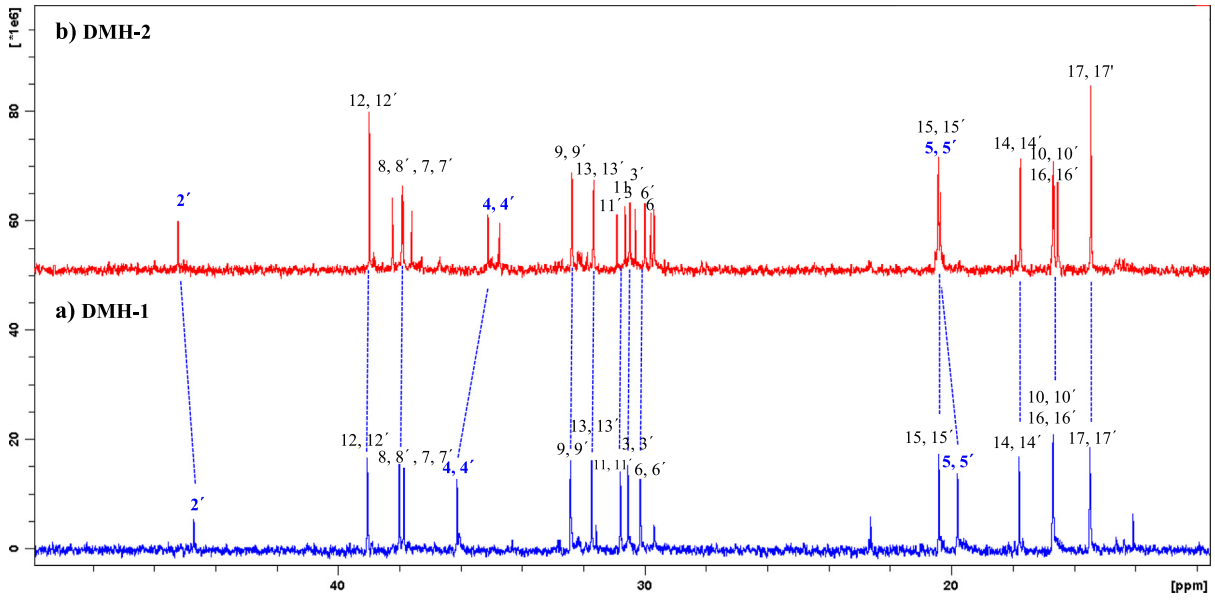

Fig. 5. 1D ^{13}C spectra of: (a) DMH-1 and (b) DMH-2.

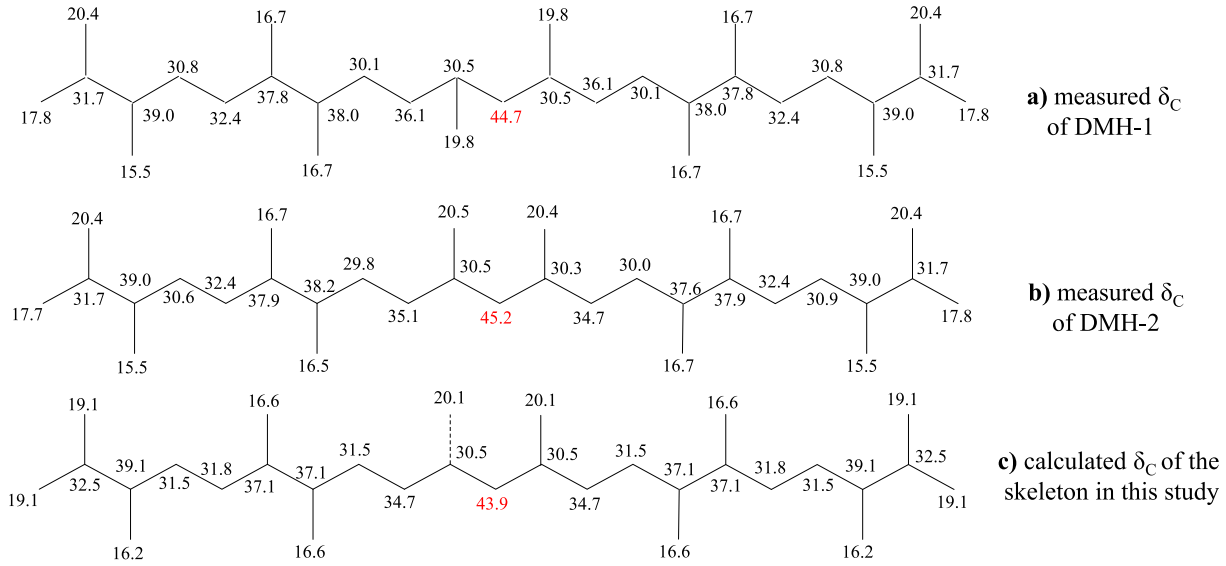

Fig. 6. Measured δ_C values of: (a) DMH-1 and (b) DMH-2, together with the δ_C values calculated by the Lindeman-Adams modeling for the new skeleton proposed in this study (c).

15.5 ppm). A pair-wise comparison of the chemical shifts between DMH-1 and DMH-2 and examination of the ^{1}H-^{13}C HMBC correlations and ^{1}H-^{1}H COSY (Fig. 4a; see Supplementary Fig. S11 for the other 2D HSQC spectrum) reveals that DMH-2 also has the same substructures **B** and **B′** identified in DMH-1. Similarly, substructures **A** and **A′** in DMH-1 can also be identified in DMH-2 as the relevant position-specific chemical shifts are very close to (but nevertheless slightly different from) those of DMH-1 (Table 1) and the left moiety of the monocyclic C_{33} sacredicene (Fig. 2b) identified in Sacred Lake sediments in Kenya (Huang et al., 1995). Thus DMH-2 can also be assigned as a decamethylhenicosane having the same structure of DMH-1.

Nevertheless the slight pairwise differences in δ_C values (of C-2′, C-4, C-4′, C-5, C-5′ in the substructures **B** and **B′**) between DMH-1 and DMH-2 (Table 1, Fig. 5) and nearly identical pairwise δ_C values for the other carbons in the substructures **A** and **A'** (Fig. 6 and Table 1) implies that the two compounds might have different configurations for the two chiral carbons C-3 and C-3′ and therefore are diastereoisomers. Since according to the ^{13}C NMR data DMH-1 is configurationally perfectly centro-symmetrical while DMH-2 is not, it is inferred that only one of the two chiral carbons C-3 and C-3′ is configurationally different between DMH-1 and DMH-2. We will show in Section 3.3 that this carbon is most likely to be C-3.

3.2. Additional support for assignment of the skeletons

To confirm the new structure proposed in this study, we made pair-wise comparison of the Lindeman-Adams modelled chemical shifts (Lindeman and Adams, 1971; refer to the Method section for parameterizing of the empirical formula). The modeled δ_C values were juxtaposed with the measured values of the two com-

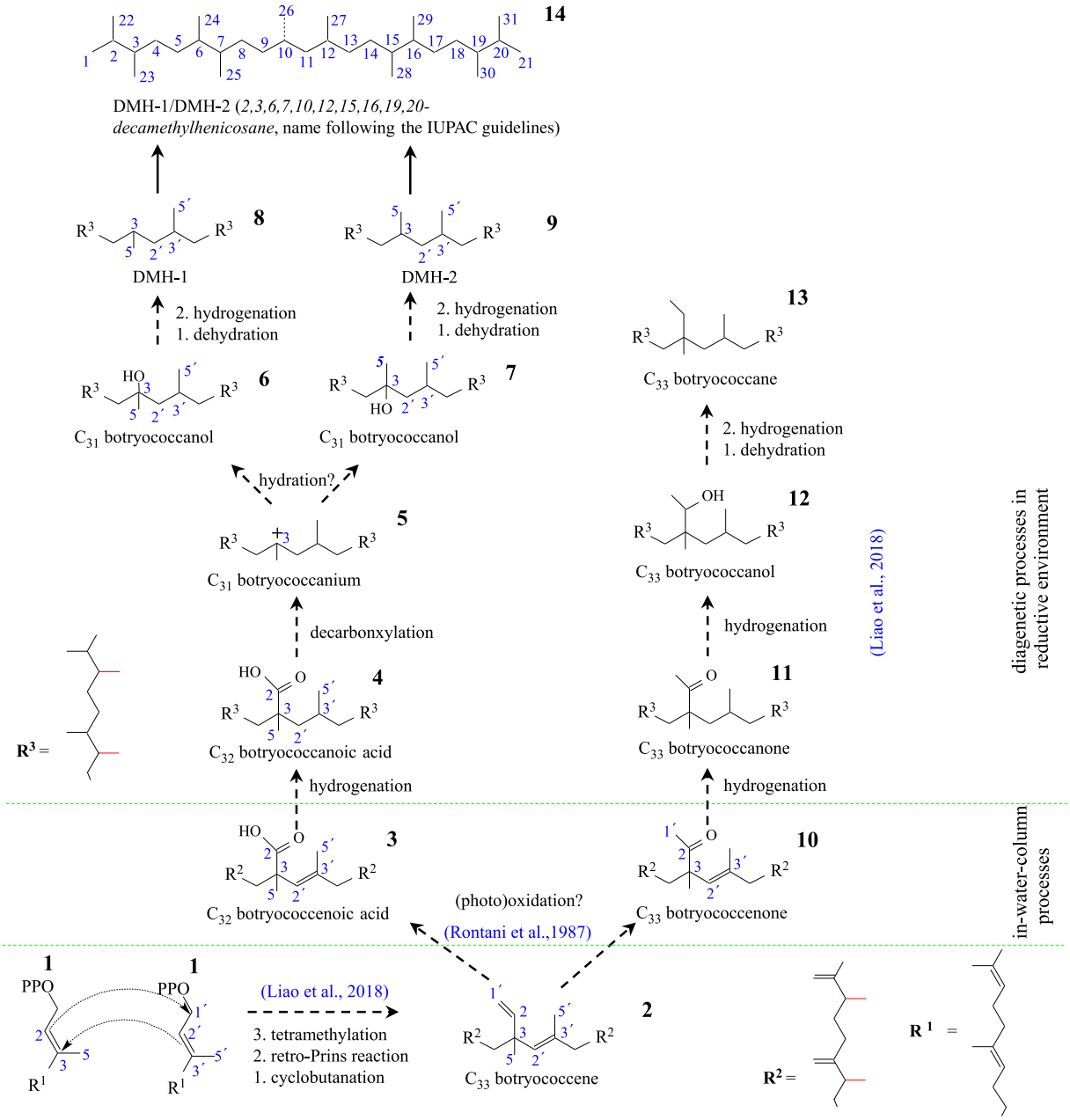

Fig. 7. Proposed pathway for the formation of the two novel isomeric DMHs. See also Liao et al. (2018) for further details for the pathway leading to the synthesis of C_{33} botryococcane (**13**) and C_{33} botryococcanone (**11**). The carbons in compounds **1**–**10** are numbered to facilitate explanation of the biosynthetic pathway and interpretation of the NMR and mass spectral data of the two DMHs, while those in compound **14** follows the IUPAC guidelines for numbering organic compounds.

pounds in Fig. 6. The measured δ_C values for both DMH-1 (Fig. 6a) and DMH-2 (Fig. 6b) were very close to the modeled values of their common skeleton (Fig. 6c). The position-specific discrepancies between the modeled and measured δ_C values for the majority of the carbons were < 1.0 ppm. Thus, the results from the Lindeman-Adams modeling strongly support the newly assigned skeleton for the two DMHs.

3.3. Geochemical pathway for the formation of the two novel polymethyl henicosanes

Since the skeletons of the two DMHs identified in the present study are very similar to that of a recent reported C_{33} botryococcane/botryococcanone (Liao et al., 2018) with a methyl group β to the quaternary carbon and since these compounds co-occurred in the same sediment sample, we propose that the two DMHs are derived from the same precursor C_{33} botryococcene (**2** in Fig. 7) from which the C_{33} botryococcane (**13** in Fig. 7) and C_{33} botryococcan-24-one (**11** in Fig. 7) are derived. As proposed in our previous work (Liao et al., 2018), the C_{33} botryococcene (**2**) skeleton was biochemically formed as a result of unusual c1′–2–3–2′ condensation (cyclobutanation) of two FPPs (farnesyl diphosphates, **1**) followed by a retro-Prins reaction and tetramethylation (see Fig. 6 of Liao et al., 2018). When present in shallow water (note that *B. braunii* is a shallow water alga), photo-mediated oxidation of **2** (Sebedio et al., 1984; Rontani et al., 1987; Kawamura and Gagosian, 1987) can convert it to an unsaturated C_{32} carboxylic acid (**3**) by cleaving the double bond of the ethenyl group connected to C-3 in compounds **1**–**9** (C-10 in **14** in Fig. 7) or an unsaturated C_{33} ketone (**10**) without breaking the ethenyl group in the light-penetrable zone. Deeper in the water column and sediments the oxidative process is expected to be gradually replaced by reduction of the double bonds in the backbones of **3** and **10**, leading to the formation of **4** (saturated acid) and **11** (saturated ketone) respectively. Decarboxylation of **4** gives rise to a hypothetical cation (**5**) with the positive charge located on C-3 (Fig. 7). Alcoholization of (**5**) can epimerize the quaternary carbon C-3, leading to the formation of two epimeric C_{31} botryococcanols (**6** and **7**). On dehydration and subsequent hydrogenation, two epimeric C_{31} alkanes (**8**, DMH-1 and **9**, DMH-2) can result. As DMH-1 is perfectly centro-symmetrical while DMH-2 is not, this may be the reason why they are base-line separated by gas chromatography (Fig. 1) even though their mass spectra and δ_C values are nearly identical or very close as diastereoisomers are known to have differential retention times in gas chromatography columns of various polarities (phases).

4. Conclusions

In the Maoming Basin oil shale sample where a C_{33} botryococcane and a C_{33} brotryococcan-24-one with a unique methyl group positioned beta to the sole quaternary carbon C-10 were identified recently (Liao et al., 2018), two epimeric C_{31} botryococcanes (DMH, 2,3,6,7,10,12,15,16,19,20-decamethylhenicosanes) with the same skeleton were identified. It is proposed that these two isomeric DMHs share the same precursor C_{33} botryococcene (formed as a result of an unusual cyclobutanation during the condensation of two farnesyl diphosphates, retro-Prins reaction and tetramethylation) with the C_{33} botryococcane and C_{33} botryococcan-24-one. Differential photo-mediated oxidation of the ethenyl group connected to the sole quaternary carbon C-10 of the C_{33} botryococcene is believed to be responsible for the formation of the co-occurring DMHs and C_{33} botryococcane/botryococcanone.

Acknowledgements

The authors thank Drs. Yankuan Tian and Wenbin Zhang for their technical help with GC–MS and pGC instrumentation and Prof. Charles Hocart for proof reading the manuscript. This work was supported by The National Key R&D Program of China (2017YFC0603102), The Strategic Priority Research Program of the Chinese Academy of Sciences (XDA14010102), The GIG-135 Shale Gas Project, China (135TP201602) and Chinese NSF grants [41673066, 41473045 and 41673045] to HL; YZ acknowledges the support of a Shaanxi Provincial Talent 100 Fellowship and a Chinese NSF grant (41773032). The work is presented in celebration of Prof. Tie-Guan Wang's 80th birthday. We thank the Associate Editor Philippe Schaeffer, and three anonymous reviewers for their helpful comments which greatly improved the manuscript. This is contribution No. IS-2585 from GIGCAS and contribution #8 from the Isotopomics in Chemical Biology group.

Appendix A. Supplementary material

Supplementary data to this article can be found online at https://doi.org/10.1016/j.orggeochem.2018.09.012.

Associate Editor–**Philippe Schaeffer**

References

Brassell, S.C., Eglinton, G., Fu, J.M., 1986. Biological marker compounds as indicators of the depositional history of the Maoming oil shale. Organic Geochemistry 10, 927–941.
Eglinton, T.I., Aluwihare, L.I., Bauer, J.E., Druffel, E.R.M., McNichol, A.P., 1996. Gas chromatographic isolation of individual compounds from complex matrices for radiocarbon dating. Analytical Chemistry 68, 904–912.
Fu, J.M., Xu, F.F., Chen, D.Y., Liu, D.H., Hu, C.Y., Jia, R.F., Xu, S.P., Brassell, A.S., Eglinton, G., 1985. Biomarker compounds of biological inputs in Maoming oil shale. Geochimica, 99–114.
Grant, D.M., Paul, E.G., 1964. Carbon-13 magnetic resonance. II. Chemical shift data for the alkanes. Journal of the American Chemical Society 86, 2984–2990.
Guy-Ohlson, D., 1992. *Botryococcus* as an aid in the interpretation of palaeoenvironment and depositional processes. Review of Palaeobotany and Palynology 71, 1–15.
Huang, Y., Murray, M., Eglinton, G., Metzger, P., 1995. Sacredicene, a novel monocyclic C_{33} hydrocarbon from sediment of Sacred Lake, a tropical freshwater lake, Mount Kenya. Tetrahedron Letters 36, 5973–5976.
Kawamura, K., Gagosian, R.B., 1987. Implications of ω-oxocarboxylic acids in the remote marine atmosphere for photo-oxidation of unsaturated fatty acids. Nature 325, 330.
Liao, J., Lu, H., Feng, Q., Zhou, Y.P., Shi, Q., Peng, P.A., Sheng, G.Y., 2018. Identification of a novel C_{33} botryococcane and C_{33} botryococcanone in the Maoming Basin, China. Organic Geochemistry 124, 103–111.
Lindeman, L.P., Adams, J.Q., 1971. Carbon-13 nuclear magnetic resonance spectrometry. Chemical shifts for the paraffins through C_9. Analytical Chemistry 43, 1245–1252.
McKirdy, D.M., Cox, R.E., Volkman, J.K., Howell, V.J., 1986. Botryococcane in a new class of Australian non-marine crude oils. Nature 320, 57–59.
Moldowan, J.M., Seifert, W.K., 1980. First discovery of botryococcane in petroleum. Journal of the Chemical Society, Chemical Communications 19, 912–914.
Özek, T., Demirci, F., 2012. Isolation of natural products by preparative gas chromatography. In: Satyajit, D.S., Lutfun, N. (Eds.), Methods in Molecular Biology, Natural Products Isolation. Humana Press, New York, pp. 275–300.
Philp, R.P., Lewis, C.A., 1987. Organic geochemistry of biomarkers. Annual Review of Earth and Planetary Sciences 15, 363–395.
Rontani, J.F., Bonin, P., Giusti, G., 1987. Mechanistic study of interactions between photo-oxidation and biodegradation of *n*-nonylbenzene in seawater. Marine Chemistry 22, 1–12.
Sebedio, J.L., Ratnayake, W.M.N., Ackman, R.G., 1984. Comparison of the reaction products of oleic acid ozonized in BCl_3^-, HCl^- and BF_3-MeOH media. Chemistry and Physics of Lipids 35, 21–28.
Volkman, J.K., 2014. Acyclic isoprenoid biomarkers and evolution of biosynthetic pathways in green microalgae of the genus *Botryococcus*. Organic Geochemistry 75, 36–47.
Zuo, H.L., Yang, F.Q., Huang, W.H., Xia, Z.N., 2013. Preparative gas chromatography and its applications. Journal of Chromatographic Science 51, 704–715.